DMD Fast Forward. Published on October 9, 2020 as DOI: 10.1124/dmd.120.000163
This article has not been copyedited and formatted. The final version may differ from this version.

In Vitro Hepatic Uptake in Human and Monkey Hepatocytes in the Presence and Absence of Serum Protein and Its *In Vitro* to *In Vivo* Extrapolation

Xiaomin Liang, Yeojin Park, Natalie DeForest, Jia Hao, Xiaofeng Zhao, Congrong Niu, Kelly Wang, Bill Smith and Yurong Lai

Drug Metabolism, Gilead Sciences Inc., Foster City, CA 94404

DMD Fast Forward. Published on October 9, 2020 as DOI: 10.1124/dmd.120.000163
This article has not been copyedited and formatted. The final version may differ from this version.

Running Title Page

Hepatic uptake in human and monkey hepatocytes and its IVIVE

Corresponding author and contact information:

Yurong Lai, PhD;
Drug Metabolism, Gilead Sciences Inc. 333 Lakeside Dr. Foster City, CA 94404
TEL: 650-522-1629; yurong.lai@gilead.com

Xiaomin Liang, PhD (co-corresponding author)

Drug Metabolism, Gilead Sciences Inc. 333 Lakeside Dr. Foster City, CA 94404
TEL: 650-653-9257; Xiaomin.Liang@gilead.com

Number of tables: 4
Number of figures: 3
Number of references: 37

Number of words:
Abstract: 249
Introduction: 674
Discussion: 1090

Abbreviations:

CL, clearance; CL_{int}, intrinsic clearance; $CL_{u,int}$, unbound intrinsic clearance; CYP, cytochrome P450; DDI, drug-drug interactions; fu, unbound fraction; IVIVE, *in vitro* to *in vivo* extrapolation; KHB, Krebs-Henseleit buffer; LC-MS/MS, liquid chromatography–tandem mass spectrometry; OATP, organic anion transporting polypeptides; PK, pharmacokinetics; PBPK, physiologically-based pharmacokinetics model; RED, rapid equilibrium dialysis; SD, standard deviation; SF, scaling factor

DMD Fast Forward. Published on October 9, 2020 as DOI: 10.1124/dmd.120.000163
This article has not been copyedited and formatted. The final version may differ from this version.

Abstract

It is well documented that human hepatic clearance based on *in vitro* metabolism or transporter assays systematically resulted in underprediction; therefore, large empirical scalars are often needed in either static or physiologically based pharmacokinetic (PBPK) models to accurately predict human pharmacokinetics (PK). In our current investigation, we assessed hepatic uptake ($CL_{int,uptake}$) in hepatocyte suspension in Krebs-Henseleit buffer (KHB) in the presence and absence of serum. The results showed that the unbound intrinsic active CL ($CL_{u,int,active}$) values obtained by normalizing the unbound fraction in the buffer containing 10% serum were generally higher than the $CL_{u,int,active}$ obtained directly from protein free buffer, suggesting "protein-facilitated" uptake. The differences of $CL_{u,int,active}$ in the buffer with and without protein ranged from 1 to 925 folds and negatively correlated to the unbound serum binding of OATP substrates. When using the uptake values obtained from buffer containing serum versus serum-free buffer, the median of scaling factors (SFs) for $CL_{u,int,active}$ reduced from 24.2 to 4.6 and 22.7 to 7.1 for human and monkey respectively, demonstrating the improvement of *in-vitro-to-in-vivo* extrapolation (IVIVE) in a PBPK model. Furthermore, $CL_{u,int,active}$ were significantly higher in monkey hepatocytes than that in human, and the species differences appeared to be compound-dependent. Scaling-up *in vitro* uptake values derived in assays containing species-specific serum can compensate the species-specific variabilities when using cynomolgus monkey as a probe animal model. Incorporating SFs calibrated in monkey and together with scaled *in vitro* data can be a reliable approach for the prospective human PK prediction in early drug discovery.

DMD Fast Forward. Published on October 9, 2020 as DOI: 10.1124/dmd.120.000163
This article has not been copyedited and formatted. The final version may differ from this version.

Significance Statement

We investigated the protein effect on hepatic uptake in human and monkey hepatocytes and improved the IVIVE using parameters obtained from the incubation in the present of serum protein. In addition, significantly higher active uptake clearances were observed in monkey hepatocytes than in human, and the species differences appeared to be compound-dependent. The PBPK model that incorporates SFs calibrated in monkey and together with scaled *in vitro* human data can be a reliable approach for the prospective human PK prediction.

DMD Fast Forward. Published on October 9, 2020 as DOI: 10.1124/dmd.120.000163
This article has not been copyedited and formatted. The final version may differ from this version.

Introduction

Accurately predicting hepatic clearance is essential for ranking and optimizing new chemical entities in the current drug discovery and development practices; furthermore, it is critically needed for understanding potential oral bioavailability, evaluating drug-drug interactions (DDIs) and determining doses in first-in-man trials. As systemic clearance (CL) are fundamental pharmacokinetic (PK) parameters for human dose projection, discovery of bioavailable and metabolically stable small molecule drug candidates are ideal goals in early PK optimization. Prediction of systemic clearance for drug candidates by major elimination organ liver is more involved. Over the past two decades, many empirical and physiologically-based approaches have been developed for human CL prediction (Ito and Houston, 2005; Chiba et al., 2009). For example, *in vitro* metabolic stability assays using liver derived systems such as liver microsomes, cytosols, and hepatocytes are routinely used for assessing enzyme stability in the early discovery stage as a high-throughput tool to select metabolically stable molecules in pharmaceutical companies (Obach et al., 1997). The rationale of these approaches is that the liver preparations prepared from human or preclinical species can reserve the enzyme activities and should reasonably represent *in vivo* clearance.

Recently, increasing recognition was given for the transporter-mediated clearance in the role on affecting drug bioavailability (first-pass hepatic extraction) and elimination. Many pharmacogenomics and DDI studies in organic anion transporting polypeptides (OATP) substrates showed transporter-mediated clearance affecting systemic drug exposure (Lai et al., 2010; Lai et al., 2012; El-Kattan et al., 2016; Yee et al., 2018). Incorporating transporter-mediated CL in the prediction of overall hepatic CL, also known as the extended clearance concept, was first introduced by Sirianni and

DMD Fast Forward. Published on October 9, 2020 as DOI: 10.1124/dmd.120.000163
This article has not been copyedited and formatted. The final version may differ from this version.

Pang and extensively investigated by other research groups (Sirianni and Pang, 1997; Kunze et al., 2015; Patilea-Vrana and Unadkat, 2016; Benet et al., 2018). Currently, a range of *in vitro* tools with increasing sophistication of transporter expressions are used to characterize transporter-mediated CL parameters for human PK prediction. Among the *in vitro* systems, hepatocytes with expression of transporter and enzyme proteins that mimic *in vivo* are often preferred to estimate *in vitro* hepatic uptake CL in suspended, plated, and sandwich-cultured hepatocytes formats. However, the discrepancies in IVIVE e.g. under predicting *in vivo* hepatic uptake CL are concerns that merited further investigations (Jones et al., 2012; Barton et al., 2013). Commonly large empirical scaling factors (SFs) were applied for transporter-mediated CL to fit *in vivo* human PK (Jones et al., 2012). The need of large empirical SFs for IVIVE also holds true in preclinical species (Watanabe et al., 2009; Morse et al., 2017; De Bruyn et al., 2018). The SFs appeared to be compound-dependent and the highly protein-bound compounds tended to have larger SFs (Jones et al., 2012; Morse et al., 2017; De Bruyn et al., 2018). Over the past years, various efforts are made to reduce the IVIVE SFs through optimizing *in vitro* methodologies such as to measure the difference of transporter expressions between *in vitro* and *in vivo* (Li et al., 2010), to incorporate human serum protein (Bowman et al., 2019; Kim et al., 2019), or to establish a "universal" SF from an internal/local *in vitro* system for laboratory specific parameters (De Bruyn et al., 2018). In our current investigation, hepatic uptake assays were conducted in suspension human and monkey hepatocytes in the presence or absence of their respective serum to elucidate the impact of protein on the active uptake for known OATPs substrates. Species differences of $CL_{int,uptake}$ between human and

DMD Fast Forward. Published on October 9, 2020 as DOI: 10.1124/dmd.120.000163
This article has not been copyedited and formatted. The final version may differ from this version.

monkey hepatocytes were also evaluated in the presence of serum protein. Additionally, a PBPK model was developed to obtain SFs from the IVIVE in monkey and human. Our comprehensive investigation on species differences in hepatic uptake for 15 OATP substrates provided insightful information for the future usage of cynomolgus monkey as probe animal model for SFs to predict human PK. Furthermore, the extensive analysis of IVIVE using compounds with a broader ranges of protein binding demonstrated the need of incorporating the protein-facilitated uptake for the human PK prediction.

Materials and Methods

Materials

Pitavastatin calcium was purchased from Fisher Scientific Company, LLC (Pittsburgh, PA). Bosentan hydrate, danoprevir, labetolol, repaglinide, valsartan, maraviroc, telmisartan, cerivastatin sodium, fluvastatin sodium, pravastatin sodium, atorvastatin calcium, rosuvastatin calcium, bucetin, warfarin, silicone oil, and mineral oil were purchased from Sigma-Aldrich, Inc. (St. Louis, MO). Grazoprevir was purchased from American Radiolabeled Chemicals, Inc. (St. Louis, MO). Sorafenib was purchased from Selleck Chemicals (Houston, TX). Asunaprevir were synthesized in house. Cryopreserved human (lot #: XPM, YTW, and PZA) (Supplemental Table S1), cynomolgus monkey (lot #: PNC, VNV, and UHK) hepatocytes (Supplemental Table S2), In VitroGRO HT medium, and Krebs-Henseleit Buffer (KHB) were obtained from BioIVT (Hicksville, NY). Cynomolgus monkey serum was purchased from Innovative Research Inc. (Novi, MI). Human serum was obtained from Corning Inc. (Corning, NY).

DMD Fast Forward. Published on October 9, 2020 as DOI: 10.1124/dmd.120.000163
This article has not been copyedited and formatted. The final version may differ from this version.

Hepatic Uptake Studies in Cryopreserved Human and Cynomolgus Monkey Hepatocytes

Total 15 known OATP substrates were selected for the hepatic uptake assays. The *in vitro* hepatic uptake clearance was evaluated in three different lots of hepatocytes for each species at a single concentration. Besides repaglinide (dosed at 0.1 µM), other 14 compounds were dosed at 1 µM in this study. Human hepatocyte lot, XPM, and monkey hepatocyte lot, UHK, were used in experiments to assess the impact of serum protein on the hepatic uptake. Uptake studies were conducted in suspended hepatocytes using oil-spin method as previously described (Kimoto et al., 2011; Morse et al., 2015). In brief, cryopreserved hepatocytes were thawed at 37 °C and immediately suspended in In VitroGro-HT medium. The hepatocytes were centrifuged at 50 g for 4 minutes at 4 °C. After centrifuging, the cells were gently resuspended in ice-cold KHB buffer. Cell viability was determined by trypan blue staining. The cell viability of hepatocyte lots used in this study exceeded 80%. The hepatocytes were diluted to 2 million cells/mL in KHB with 10% (v/v) human and cynomolgus monkey serum, respectively. The compounds (1000X concentration in DMSO) were diluted in uptake buffer (KHB with or without 10% human or cynomolgus monkey serum). Prior to uptake experiments, cell suspension and uptake buffer containing 2X substrate concentration was incubated at warm or ice-cold water bath for 10 minutes to reach the uptake temperature at 37 °C or 4 °C. Uptake assays were initiated by adding the uptake buffer to cell suspension (1:1 in v/v), which resulted in 1X final substrate concentration in a cell density of 1 million cells/mL. For the uptake studies, all compounds were performed in 1 µM final concentration, except repaglinide which had final concentration of 0.1 µM. The

DMD Fast Forward. Published on October 9, 2020 as DOI: 10.1124/dmd.120.000163
This article has not been copyedited and formatted. The final version may differ from this version.

incubations were terminated at 0.25, 0.5, 1, 1.5, and 5 minutes by collecting100 µl of incubation mixture onto a micro centrifuge tube containing two layers preloaded. The bottom layer contained 100 µL of 3 M ammonium acetate and the upper layer contained 100 µL oil mixture of silicone oil and mineral oil (density = 1.015). The micro centrifuge tubes were immediately centrifuged at 14,000 rpm for 14 seconds in Eppendorf benchtop centrifuge. The oil layer separated the cells from the uptake buffer. Micro centrifuge tubes were immediately placed on dry ice and transferred to -80 °C freezer until analysis. The active transporter-mediated uptake was assessed at 37 °C and passive diffusion was assessed at 4 °C, assuming minimal transporter activities at 4 °C. For each batch of uptake experiment, rosuvastatin was included to monitor variations from batch to batch. The uptake assay was conducted in triplicates at each time point for all compounds. Human hepatocyte lot XPM and monkey hepatocyte lot UHK were used in the uptake study to compare the *in vitro* hepatic uptake clearance in the presence or absence of serum protein. Moreover, three donors of human (XPM, PZA, and YTW) and monkey (UHK, PNC, and VNV) hepatocytes were used to further assess the donor variability.

Liquid Chromatography–Tandem Mass Spectroscopy (LC-MS/MS) Analysis

Tips of microcentrifuge tubes containing hepatocyte pellets were cut and placed upside down in deep 96 well plates. 100 µl of deionized water was added to each well and the cells were sonicated for 10 minutes. 200 µL of 100 % acetonitrile with internal standard, labetalol, was added to the wells for compound extraction. The samples were sonicated for 10 minutes and followed by shaking on a shaker for 20 minutes. After additional 5 minutes sonication, the samples were centrifuged at 4000 rpm for 20

DMD Fast Forward. Published on October 9, 2020 as DOI: 10.1124/dmd.120.000163
This article has not been copyedited and formatted. The final version may differ from this version.

minutes at 4 °C. Standard curves for quantitation were prepared in blank hepatocyte pellets that were treated similarly to hepatocyte samples. 150 µL aliquot was transferred into 96 deep well plates and then completely dried. The samples were reconstituted in 200 µL buffer containing 20% acetonitrile and 80% water with 0.1% formic acid. The samples were vortexed and centrifuged at 3500 rpm at 4 °C for 20 minutes before LC-MS/MS analysis.

All the samples were analyzed on a Sciex Qtrap 6500 LC-MS/MS (Redwood city, CA) coupled with a Shimadzu Nexera-X2 ultra high-performance liquid chromatograph (Shimadzu Corporation, Kyoto, Japan). Ten microliters of the sample were injected onto a Waters Acquity UPLC BEH C18 column (1.7 um, 2.1 mm x 50 mm) (Milford, MA) and eluted by gradient mobile phases of 0.1% formic acid in water (A) and acetonitrile (B). The LC-MS/MS conditions for each compound were summarized in Supplemental Table S3.

Unbound Fraction in Serum Protein

Serum protein binding of 15 compounds was determined in 100% and 10% human or monkey serum by equilibrium dialysis with a Rapid Equilibrium Dialysis (RED) Device (Thermo Fisher Scientific, Rockford, IL). The DMSO stock solution of the test article was spiked into 100% or 10% (diluted in KHB buffer) human or monkey serum to a final concentration of 2 µM. 100 µL aliquot of the spiked serum was transferred to a 96-well deep-well plate as the T0 sample. Blank KHB buffer (pH 7.4, 100 µL) was added to the plate to make the matrix of 50:50 (v/v) serum:buffer. The T0 samples were incubated at 37 °C for 4 hours. The spiked samples were placed into the sample chamber (300 µL) while the KHB buffer was placed into the adjacent buffer chamber

DMD Fast Forward. Published on October 9, 2020 as DOI: 10.1124/dmd.120.000163
This article has not been copyedited and formatted. The final version may differ from this version.

(500 µL). The plate was sealed with a self-adhesive lid and incubated at 37 ºC on an orbital shaker (250 rpm) for 4 hours. The assay was carried in duplicates. At the end of the incubations, aliquots (100 µL) were taken from both the serum and buffer chambers. Blank KHB buffer (100 µL) was added to the serum samples and blank serum or 10% serum (100 µL) were added to the buffer samples. Finally, 300 µL of quench solution (50% acetonitrile and 50% methanol with 0.05% formic acid) containing internal standards (bucetin and warfarin) was added to each sample. The quenched samples were vortexed vigorously for 20 min and centrifuged at 4,000 rpm at 10°C. The supernatants were transferred to a 96-well plate and analyzed by LC/MS-MS. The % free and % recovery of test compound was calculated (Supplemental Table S4).

In Vitro Uptake Data Analysis

The intrinsic total uptake clearance ($CL_{int,uptake}$) and intrinsic passive uptake clearance ($CL_{int,passive}$) were obtained from the initial uptake rates at 37 or 4 °C, respectively. The initial uptake rates were estimated from the slopes of linear uptake phase using linear regression analysis. The intrinsic uptake clearance values were calculated by dividing the initial uptake velocity by the nominal substrate concentration. The intrinsic active uptake clearance ($CL_{int,active}$) was calculated by subtracting the $CL_{int,passive}$ from $CL_{int,uptake}$. The unbound intrinsic uptake clearance ($CL_{u,int,active}$ and $CL_{u,int,passive}$) was calculated by dividing intrinsic clearance by the measured unbound fraction in buffer containing 10% serum or 100% for study in serum free buffer.

The *in vitro* intrinsic CL values were expressed as microliters per minute per million cells. The scaled *in vivo* intrinsic clearances were calculated by multiplying hepatocellularity (125 million cells per g liver in human and 122 million cells per g liver in

DMD Fast Forward. Published on October 9, 2020 as DOI: 10.1124/dmd.120.000163
This article has not been copyedited and formatted. The final version may differ from this version.

cynomolgus monkey) and liver weight of 25.5 and 19.7 g liver per kilogram body weight in human and cynomolgus monkey, respectively. The numbers of hepatocellularity and liver weight were adapted from SimCYP (Certara Ltd. Version 17).

In Vivo Pharmacokinetic Study of Pitavastatin in Cynomolgus Monkey

PK studies were performed in cynomolgus monkeys to understand IVIVE of in vitro hepatic uptake parameters. The PK studies were performed in WuXi AppTec (Suzhou, China). All procedures were approved by an Institutional Animal Care and Use Committee. In brief, each cynomolgus monkey (n = 4 male, 3 – 5 kg) was dosed at 0.5 mg/kg in 5% DMSO/95% saline solution. Individual doses were calculated based on body weights recorded on the day of dose administration. The intravenous (I.V.) dose was administered as an approximately 30-minute infusion using a calibrated Harvard Apparatus PHD 2000 infusion pump via cephalic vein. Serial blood samples were collected via the femoral vein before dosing and at predefined time points. Blood samples were maintained on ice prior to centrifugation to obtain plasma (K_2EDTA). Centrifugation began within 1 hour of collection. Plasma samples (approximately 500 µL) were placed into a 96-well tube containing 4 µL of formic acid (the final concentration of formic acid in plasma was approximately 2%) and samples were vortex mixed. The plasma samples were analyzed using LC-MS/MS.

Physiologically Based Pharmacokinetic (PBPK) Model Analysis for *In Vivo* Hepatic Uptake Parameters

A five-compartmental liver model was adapted from previously published PBPK model for OATP substrates (Jones et al., 2012; Morse et al., 2015; Morse et al., 2017).

DMD Fast Forward. Published on October 9, 2020 as DOI: 10.1124/dmd.120.000163
This article has not been copyedited and formatted. The final version may differ from this version.

The mass balance differential equations that described previously (Jones et al., 2012; Morse et al., 2017) were employed in SAAM II (the Epsilon Group, Charlottesville, VA). The tissue partition coefficient (Kp) for each non-liver tissue was obtained from SimCYP (Certara Ltd. Version 17). A fitting procedure for pitavastatin plasma PK curves was performed to determine *in vivo* hepatic clearance parameters, which utilizes a similar procedure previously published for other OATP substrates (Jones et al., 2012; Morse et al., 2017). In brief, the scaled unbound intrinsic CL parameters calculated from the *in vitro* uptake values obtained from uptake assay using the protein free buffer or buffer containing 10% serum were used as the initial estimates. The fitted values of $CL_{u,int,active}$, $CL_{u,int,passive}$, and $CL_{u,int,bile}$ were estimated by fitting the plasma PK curve. The pitavastatin monkey plasma PK data was obtained from in-housed data and the human plasma PK data was digitalized (GetData Graph Digitizer V 2.26.0) from previous published NDA (NDA022363). The empirical scaling factors (SF) were calculated for each of $CL_{u,int,active}$ and $CL_{u,int,passive}$ by dividing the *in vitro* scaled value by the fitted value. The median of SFs across the drugs in the dataset was calculated.

Results

In Vitro Hepatic Uptake in Human and Monkey Hepatocytes in Presence or Absence of Serum Protein

The impact of serum protein on the hepatic uptake was first assessed in in suspension human and monkey hepatocytes. The hepatocytes were incubated with known OATP substrates in KHB buffer containing with or without 10% serum. The unbound serum protein fraction of OATP substrates in both 100% and 10% serum buffer was measured and data was summarized in Supplemental Table S4. All

DMD Fast Forward. Published on October 9, 2020 as DOI: 10.1124/dmd.120.000163
This article has not been copyedited and formatted. The final version may differ from this version.

compounds had good recovery numbers (> 80%). Due to sorafenib is highly bound to serum protein, the % free in 100% human or monkey serum was not able to determine. Among these OATP substrates, the serum protein binding values were highly correlated between human and monkey as R^2 values were higher than 0.9 in both assays measured in 100% serum and 10% serum containing buffer (Figure 1). The *in vitro* values of $CL_{u,int,uptake}$, $CL_{u,int,active}$, and $CL_{u,int,passive}$, for 15 OATP substrates were obtained either from the incubation with and without serum protein were summarized in Table 1. As shown in Table 1, the values of $CL_{u,int,active}$ obtained in the buffer containing 10% serum protein were generally higher than values obtained directly from the uptake in the protein free buffer in both human and monkey hepatic uptake studies. The shift was ranged from 1.5 to 924.6-fold higher in human or 1 to 878.5-fold higher in monkey, respectively. The higher fold-differences were observed in higher serum protein bound compounds. In additional, similar tread of shift was observed in $CL_{u,int,passive}$ for highly protein bound compounds. Similar observation was reported in the recent publication from other research groups (Bowman et al., 2019; Kim et al., 2019; Bowman et al., 2020). In the nonparametric spearman correlation test, the fold-differences of $CL_{u,int,passive}$ and $CL_{u,int,active}$ in both human (Figure 2A-B) and monkey hepatocytes (Figure 2C-D) were negatively correlated with the serum protein binding values.

In Vitro to *In Vivo* Extrapolation of Hepatic Uptake Clearances in PBPK Modeling

Recent publication suggested performing *in vitro* hepatic uptake studies in the presence of protein could improve the prediction of transporter-mediated hepatic clearance (Bowman et al., 2019; Kim et al., 2019). In our current study, the impact of addition of serum protein in the uptake assay on the improvement of IVIVE was further

DMD Fast Forward. Published on October 9, 2020 as DOI: 10.1124/dmd.120.000163
This article has not been copyedited and formatted. The final version may differ from this version.

investigated in PBPK modeling. The *in vivo* intrinsic CL fitted parameters were estimated by human or monkey PBPK models reported previously (Jones et al., 2012; Morse et al., 2015; Morse et al., 2017), except for pitavastatin. The IVIVE of pitavastatin in monkey and human was performed by a curve fit of plasma PK using in-house PBPK model adapted from previously published models (Jones et al., 2012; Morse et al., 2017) (Figure 3). As shown in Table 2, the SFs for $CL_{u,int,passive}$ ranged from 0.1 to 7.7 with the median of 0.8 in human or the median of 0.9 in monkey when using the scaled *in vitro* parameters obtained from the incubation without serum protein, while the SFs ranged from 0.1 to 10.3 with the median of 0.5 in human or the median of 0.6 in monkey when applying the *in vitro* parameters from the incubation with 10% serum. On the other hand, the SFs for $CL_{u,int,active}$ ranged from 7.3 to 106 with the median of 24.2 in human or 22.7 in monkey when *in vitro* parameters acquired from the incubation in serum free buffer. As expected, the SFs for $CL_{u,int,active}$ were ranged from 2.3 to 23.7 with the median of 4.6 in human or 7.1 in monkey when the model incorporated the scaled *in vitro* parameters obtained from the incubation in buffer containing 10% serum. The results indicated that the empirical SFs were significantly larger when using *in vitro* parameters obtained in the serum free buffer, as compared to the parameters obtained from the incubation with serum protein added.

Differences of Hepatic Uptake Clearance in Human and Monkey Hepatocytes for Known OATP Substrates

To assess the species differences and donor variability in transporter-mediated uptake in hepatocytes between human and cynomolgus monkey, hepatic uptake assays were conducted in two additional donors for each species. The *in vitro* uptake assays

DMD Fast Forward. Published on October 9, 2020 as DOI: 10.1124/dmd.120.000163
This article has not been copyedited and formatted. The final version may differ from this version.

were performed in the buffer with 10% respective human and monkey serum. The values of *in vitro* hepatic uptake clearance were then adjusted by the fraction of unbound in 10% serum buffer. The values of $CL_{u,int,uptake}$, $CL_{u,int,active}$, and $CL_{u,int,passive}$ for each donor in human and monkey hepatocytes were summarized in the Table 3. In general, the values of uptake clearances obtained from different lots were with 2-fold range and the values of $CL_{u,int,passive}$ between human and monkey hepatocytes were comparable (two-tailed p = 0.4 in Wilcoxon paired nonparametric test). One the other side, the $CL_{u,int,active}$ in monkey hepatocytes were about 2-fold higher than in human hepatocytes (two-tailed p = 0.0001 in Wilcoxon paired nonparametric test).

Discussion

As a general practice, *in vitro* metabolic stability is routinely examined using hepatic preparations and hepatic uptake studies in suspended, plated, and sandwich-cultured hepatocytes are used to estimate hepatic transporter-mediated uptake clearance in early drug discovery. *In vitro* parameters obtained are then scaled to *in vivo* clearances by multiplying the hepatocellularlarity and liver weight (Li et al., 2009; Bi et al., 2012). While this physiologically-based IVIVE appears to be the best approach, systematic underprediction is a well-known issue (Yamagata et al., 2017; Bowman and Benet, 2019). To bridge the gap of transporter-mediated clearance IVIVE, empirically-derived SFs were widely utilized to parametrize the transporter-associated clearance such as $CL_{u,int,active}$, $CL_{u,int,passive}$, and $CL_{u,int,bile}$. In addition, confidence in the prediction is low for the compounds that are less permeable and subject to transporter substrates with high protein binding (Jones et al., 2012; Jones et al., 2015; Yamagata et al., 2017; De Bruyn et al., 2018). Recently, Kim et al. showed that the $CL_{u,int,active}$ increases in the

DMD Fast Forward. Published on October 9, 2020 as DOI: 10.1124/dmd.120.000163
This article has not been copyedited and formatted. The final version may differ from this version.

presence of human serum albumin for 11 highly protein bound drugs (Kim et al., 2019). As a result, an improved IVIVE for 11 OATP substrates was achieved using uptake parameters obtained from the incubation in the presence of human serum protein (Kim et al., 2019). Moreover, Bowman et al. also showed similar results by doing uptake studies in the presence of 100% plasma for high protein binding substrates such as atorvastatin and pitavastatin in fresh isolated rat hepatocytes (Bowman et al., 2019). Collectively, a theory of “protein-facilitated” or “transporter-induced protein binding shift” uptake was proposed for the improved IVIVE (Baik and Huang, 2015; Zhang et al., 2015; Miyauchi et al., 2018; Bowman et al., 2019). In the present investigation, we measured the *in vitro* $CL_{int,uptake}$ in suspension hepatocytes in the buffer with or without 10% human or cynomolgus monkey serum. As expected, *in vitro* $CL_{u,int,active}$ obtained from the incubation in the buffer containing 10% serum were greatly increased compared to the $CL_{u,int,active}$ obtained from the incubation in protein free buffer (Table 1). The fold-differences highly correlated with the protein binding (Figure 2), with particularly larger differences were observed for the drugs that were highly protein bound, such as sorafenib (925 folds), asunaprevir (23 folds), and valsartan (15 folds) in human hepatocytes. Similar results were observed in monkey hepatocytes. Therefore, the SFs for $CL_{u,int,active}$ were significantly lower for each compound especially for highly protein bound drugs, when using scaled $CL_{u,int,active}$ from the incubation in the buffer containing 10% serum protein (Table 2). As expected, less fold shift was observed for lower protein binding compounds such as rosuvastatin and pravastatin. Interestingly, the larger empirical SFs were needed for pravastatin IVIVE in both human and in monkey, which is consistent with the recent report by Bruyn et al. (De Bruyn et al.,

DMD Fast Forward. Published on October 9, 2020 as DOI: 10.1124/dmd.120.000163
This article has not been copyedited and formatted. The final version may differ from this version.

2018). These data suggested that uptake clearance of pravastatin was significantly underestimated *in vitro*, even in the incubation with serum protein. Pravastatin has been reported to be a substrate for many other uptake and efflux transporters (Table 4) and the protein binding is low (57% free in human serum) (Supplemental Table S4). In addition, renal elimination also significantly contributes to overall systemic clearance (pravastatin drug label). In addition, previous publication suggested addition of protein had effect on both V_{max} and K_m of transport kinetics (Bowman et al., 2019; Kim et al., 2019; Bowman et al., 2020). In present study, only single concentration was used in the uptake assay. Thus, further studies on the contribution of each transporter, the preservation of transporter function in cryopreserved hepatocytes, the changes of V_{max} and K_m in the presence of serum protein, and IVIVE involved various elimination pathways are warranted. Nevertheless, the empirical SFs in the present investigation appeared to be comparable with the literature SFs using uptake values obtained from the incubation with 5% human serum albumin (Kim et al., 2019).

Moreover, recent published studies (Bowman et al., 2019; Bowman et al., 2020) and as well as our present investigation showed the passive diffusion also increased with addition of protein in the uptake experiments as a result of higher values of $CL_{u,int,passive}$ observed, especially for highly protein bound compounds (Table 1 and Figure 2). The data suggested protein affected both active uptake and passive diffusion. One possible mechanism is that changing the interaction between the binding to the serum protein and nonspecific binding to the cells membrane when adding protein to uptake buffer. For example, the serum protein (with compound highly bound) may bind to cell membrane during the incubation and the binding of serum protein on the cell

DMD Fast Forward. Published on October 9, 2020 as DOI: 10.1124/dmd.120.000163
This article has not been copyedited and formatted. The final version may differ from this version.

membrane may be not fully washed with buffer or separated by the oil layer. When we lysed cells, the cell membrane fraction was included in the analysis. Such contamination may confound the results. Other possible reason is that the solutes in plasma/serum may change the osmotic pressure of cell membrane, which may be different in protein free buffer. As previous reports, even in an isotonic environment, animal cells face a problem in maintaining cell volume (Lodish et al., 2000). The solutes and other molecules in the plasma/serum may affect the function of ATP- Na^+/K^+ pump and ion movements and sequentially change the cell volume and surface area. As the intrinsic clearance of passive diffusion can be defined as the permeability-surface area (PS), the change of cell volume and surface area may affect passive diffusion. Collectively, the mechanism of protein affecting passive diffusion remain unknown. Further investigation is needed in this field.

Many studies showed that a “middle-out” approach can reasonably capture clinical PK profiles and predict clinical DDIs when using PBPK models (Varma et al., 2012; Barton et al., 2013; Duan et al., 2017). Unfortunately, human PK data are unlikely available during drug discovery and early development phase, which limit to the application of the “middle-out” modeling. As such, to incorporate transporter-mediated clearance for human PK prediction during compound selection and engage PBPK modeling along lead optimization, one of critical options is to derive SFs from preclinical species and apply the SFs for prospective human PK prediction. However, concerns remain when translating preclinical animal data to human due to poor protein homology for drug transporters. Being a species with high degrees homology to human OATP isoforms (Shen et al., 2013; Kimoto et al., 2017; De Bruyn et al., 2018), cynomolgus

DMD Fast Forward. Published on October 9, 2020 as DOI: 10.1124/dmd.120.000163
This article has not been copyedited and formatted. The final version may differ from this version.

monkey become a promising preclinical species that can be used in transporter characterization to bridge the gaps of human IVIVE. As such, we further characterized hepatic uptake in human and monkey hepatocytes under the condition in the buffer containing 10% serum. Three hepatocyte lots were included in the uptake studies for each species to evaluate variation among difference lots or donors. As shown in Table 3, among 15 known OATP and other transporter substrates (Table 4), the uptake values in different lots were generally within 2-fold. Although the binding to hepatocytes cannot be ignored in the incubation, the binding to the hepatocytes should be similar in both human and monkey. After the correction of serum binding, the values of *in vitro* $CL_{u,int,passive}$ were generally comparable between human and monkey. On the other hand, *in vitro* $CL_{u,int,active}$ in monkey was signifyingly higher than in human (> 2 fold) and appeared to be compound dependent (Table 3). It is worth noting that the SFs of $CL_{u,int,passive}$ for bosentan and rosuvastatin in monkey were higher than in human, although the SFs of $CL_{u,int,active}$ were comparable (Table 2). As the data of protein binding in 10% serum buffer (Supplemental Table S4) and the values of *in vitro* $CL_{u,int,passive}$ were comparable in human and monkey for both bosentan and rosuvastatin, therefore, the large difference of SFs in $CL_{u,int,passive}$ between human and monkey was less likely due to *in vitro* experiments. For bosentan and rosuvastatin, the PBPK modeling of human and monkey were performed by two different groups. In addition, the curve fitting in human PBPK solely relied on plasma PK data (Jones et al., 2012) while both liver and plasma data were used in curve fitting in monkey model (Morse et al., 2017). Different models and fitting process may contribute to the different SFs of $CL_{u,int,passive}$ obtained in human and monkey for bosentan and rosuvastatin. In the

DMD Fast Forward. Published on October 9, 2020 as DOI: 10.1124/dmd.120.000163
This article has not been copyedited and formatted. The final version may differ from this version.

case of pitavastatin, both human and monkey PBPK models were developed in-house for plasma PK curve fitting, the SFs of $CL_{u,int,passive}$ and $CL_{u,int,active}$ were comparable between human and monkey (Table 2). Although the serum protein binding data were correlated well among these 15 compounds between human and monkey (Figure 1), other study observed poor correlation of protein binding between preclinical species and human (Lombardo et al., 2013). In this regard, when interpreting protein facilitated uptake clearance and translating from preclinical animal to human, it is recommended to consider the species difference in protein binding and as well as the difference in transport kinetics. Nevertheless, since overall difference of hepatic uptake obtained from the incubation in the buffer containing serum proteins incorporates multiple species-specific variables to compensate the complexities affecting the hepatic uptake such as difference of transporter expression, the relative contribution of each transporter, substrate affinity of each transporter and protein binding, SFs derived from the IVIVE in monkey can be reliably used in PBPK models for prospective human PK prediction.

In summary, the IVIVE of transporter-mediated clearance were significantly improved when using hepatic uptake parameters obtained from the incubation with serum protein in the uptake experiments. The species differences were found in hepatic uptakes between money and human hepatocytes for 15 known OATPs substrates and the difference appeared to be substrate-dependent. As compound advancing during drug discovery and early development, cynomolgus monkeys can be served as a good preclinical animal model to probe the SFs of transporter-mediated uptake parameters for prospective human PK prediction.

DMD Fast Forward. Published on October 9, 2020 as DOI: 10.1124/dmd.120.000163
This article has not been copyedited and formatted. The final version may differ from this version.

DMD Fast Forward. Published on October 9, 2020 as DOI: 10.1124/dmd.120.000163
This article has not been copyedited and formatted. The final version may differ from this version.

Acknowledgments

We thank Drs. Bernard Murray and Yang Song for helpful scientific discussions

Authorship Contributions

Participated in research design: X. Liang, Y. Lai, B. Smith

Conducted experiments: X. Liang, Y. Park, J. Hao, X. Zhao, N. DeForest, C. Niu, K. Wang

Performed data analysis: X. Liang, Y. Park, J. Hao, X. Zhao, Y. Lai

Contribute to manuscript writing: X. Liang, Y. Park, Y. Lai

Reference:

Baik J and Huang Y (2015) Transporter-induced protein binding shift (TIPBS) hypothesis and modeling. *Poster in 20th North American ISSX Meeting* **Orlando:**October 2015.

Barton HA, Lai Y, Goosen TC, Jones HM, El-Kattan AF, Gosset JR, Lin J, and Varma MV (2013) Model-based approaches to predict drug-drug interactions associated with hepatic uptake transporters: preclinical, clinical and beyond. *Expert Opin Drug Metab Toxicol* **9:**459-472.

Benet LZ, Bowman CM, Liu S, and Sodhi JK (2018) The Extended Clearance Concept Following Oral and Intravenous Dosing: Theory and Critical Analyses. *Pharm Res* **35:**242.

Bi YA, Kimoto E, Sevidal S, Jones HM, Barton HA, Kempshall S, Whalen KM, Zhang H, Ji C, Fenner KS, El-Kattan AF, and Lai Y (2012) In vitro evaluation of hepatic transporter-mediated clinical drug-drug interactions: hepatocyte model optimization and retrospective investigation. *Drug Metab Dispos* **40:**1085-1092.

Bowman CM and Benet LZ (2019) In Vitro-In Vivo Extrapolation and Hepatic Clearance-Dependent Underprediction. *J Pharm Sci* **108:**2500-2504.

Bowman CM, Chen E, Chen L, Chen YC, Liang X, Wright M, Chen Y, and Mao J (2020) Changes in Organic Anion Transporting Polypeptide Uptake in HEK293 Overexpressing Cells in the Presence and Absence of Human Plasma. *Drug Metab Dispos* **48:**18-24.

Bowman CM, Okochi H, and Benet LZ (2019) The Presence of a Transporter-Induced Protein Binding Shift: A New Explanation for Protein-Facilitated Uptake and Improvement for In Vitro-In Vivo Extrapolation. *Drug Metab Dispos* **47:**358-363.

Chiba M, Ishii Y, and Sugiyama Y (2009) Prediction of hepatic clearance in human from in vitro data for successful drug development. *AAPS J* **11:**262-276.

De Bruyn T, Ufuk A, Cantrill C, Kosa RE, Bi YA, Niosi M, Modi S, Rodrigues AD, Tremaine LM, Varma MVS, Galetin A, and Houston JB (2018) Predicting Human Clearance of Organic Anion Transporting Polypeptide Substrates Using Cynomolgus Monkey: In Vitro-In Vivo Scaling of Hepatic Uptake Clearance. *Drug Metab Dispos* **46:**989-1000.

Duan P, Zhao P, and Zhang L (2017) Physiologically Based Pharmacokinetic (PBPK) Modeling of Pitavastatin and Atorvastatin to Predict Drug-Drug Interactions (DDIs). *Eur J Drug Metab Pharmacokinet* **42:**689-705.

El-Kattan AF, Varma MV, Steyn SJ, Scott DO, Maurer TS, and Bergman A (2016) Projecting ADME Behavior and Drug-Drug Interactions in Early Discovery and Development: Application of the Extended Clearance Classification System. *Pharm Res* **33:**3021-3030.

Ito K and Houston JB (2005) Prediction of human drug clearance from in vitro and preclinical data using physiologically based and empirical approaches. *Pharm Res* **22:**103-112.

Jones HM, Barton HA, Lai Y, Bi YA, Kimoto E, Kempshall S, Tate SC, El-Kattan A, Houston JB, Galetin A, and Fenner KS (2012) Mechanistic pharmacokinetic modeling for the prediction of transporter-mediated disposition in humans from sandwich culture human hepatocyte data. *Drug Metab Dispos* **40:**1007-1017.

Jones HM, Chen Y, Gibson C, Heimbach T, Parrott N, Peters SA, Snoeys J, Upreti VV, Zheng M, and Hall SD (2015) Physiologically based pharmacokinetic modeling in drug discovery and development: a pharmaceutical industry perspective. *Clin Pharmacol Ther* **97:**247-262.

Kim SJ, Lee KR, Miyauchi S, and Sugiyama Y (2019) Extrapolation of In Vivo Hepatic Clearance from In Vitro Uptake Clearance by Suspended Human Hepatocytes for Anionic Drugs with High Binding to Human Albumin: Improvement of In Vitro-to-In Vivo Extrapolation by Considering the "Albumin-Mediated" Hepatic Uptake Mechanism on the Basis of the "Facilitated-Dissociation Model". *Drug Metab Dispos* **47:**94-103.

Kimoto E, Bi YA, Kosa RE, Tremaine LM, and Varma MVS (2017) Hepatobiliary Clearance Prediction: Species Scaling From Monkey, Dog, and Rat, and In Vitro-In Vivo Extrapolation of Sandwich-Cultured Human Hepatocytes Using 17 Drugs. *J Pharm Sci* **106:**2795-2804.

Kimoto E, Chupka J, Xiao Y, Bi YA, and Duignan DB (2011) Characterization of digoxin uptake in sandwich-cultured human hepatocytes. *Drug Metab Dispos* **39:**47-53.

Kunze A, Poller B, Huwyler J, and Camenisch G (2015) Application of the extended clearance concept classification system (ECCCS) to predict the victim drug-drug interaction potential of statins. *Drug Metabol Personal Ther* **30:**175-188.

Lai Y, Sampson KE, and Stevens JC (2010) Evaluation of drug transporter interactions in drug discovery and development. *Comb Chem High Throughput Screen* **13:**112-134.

Lai Y, Varma M, Feng B, Stephens JC, Kimoto E, El-Kattan A, Ichikawa K, Kikkawa H, Ono C, Suzuki A, Suzuki M, Yamamoto Y, and Tremaine L (2012) Impact of drug transporter pharmacogenomics on pharmacokinetic and pharmacodynamic variability - considerations for drug development. *Expert Opin Drug Metab Toxicol* **8:**723-743.

Li N, Bi YA, Duignan DB, and Lai Y (2009) Quantitative expression profile of hepatobiliary transporters in sandwich cultured rat and human hepatocytes. *Mol Pharm* **6:**1180-1189.

Li N, Singh P, Mandrell KM, and Lai Y (2010) Improved extrapolation of hepatobiliary clearance from in vitro sandwich cultured rat hepatocytes through absolute quantification of hepatobiliary transporters. *Mol Pharm* **7:**630-641.

Lodish H, Berk A, Zipursky S, Matsudaira P, Baltimore D, and Darnell J (2000) Osmosis, Water Channels, and the Regulation of Cell Volume, in: *Molecular Cell Biology*, W. H. Freeman, New York.

Lombardo F, Waters NJ, Argikar UA, Dennehy MK, Zhan J, Gunduz M, Harriman SP, Berellini G, Liric Rajlic I, and Obach RS (2013) Comprehensive assessment of human pharmacokinetic prediction based on in vivo animal pharmacokinetic data, part 2: clearance. *J Clin Pharmacol* **53:**178-191.

Miyauchi S, Masuda M, Kim SJ, Tanaka Y, Lee KR, Iwakado S, Nemoto M, Sasaki S, Shimono K, Tanaka Y, and Sugiyama Y (2018) The Phenomenon of Albumin-Mediated Hepatic Uptake of Organic Anion Transport Polypeptide Substrates: Prediction of the In Vivo Uptake Clearance from the In Vitro Uptake by Isolated Hepatocytes Using a Facilitated-Dissociation Model. *Drug Metab Dispos* **46:**259-267.

Morse BL, Cai H, MacGuire JG, Fox M, Zhang L, Zhang Y, Gu X, Shen H, Dierks EA, Su H, Luk CE, Marathe P, Shu YZ, Humphreys WG, and Lai Y (2015) Rosuvastatin Liver Partitioning in Cynomolgus Monkeys: Measurement In Vivo and Prediction Using In Vitro Monkey Hepatocyte Uptake. *Drug Metab Dispos* **43:**1788-1794.

Morse BL, MacGuire JG, Marino AM, Zhao Y, Fox M, Zhang Y, Shen H, Griffith Humphreys W, Marathe P, and Lai Y (2017) Physiologically Based Pharmacokinetic Modeling of Transporter-Mediated Hepatic Clearance and Liver Partitioning of OATP and OCT Substrates in Cynomolgus Monkeys. *AAPS J* **19:**1878-1889.

Obach RS, Baxter JG, Liston TE, Silber BM, Jones BC, MacIntyre F, Rance DJ, and Wastall P (1997) The prediction of human pharmacokinetic parameters from preclinical and in vitro metabolism data. *J Pharmacol Exp Ther* **283:**46-58.

Patilea-Vrana G and Unadkat JD (2016) Transport vs. Metabolism: What Determines the Pharmacokinetics and Pharmacodynamics of Drugs? Insights From the Extended Clearance Model. *Clin Pharmacol Ther* **100:**413-418.

Shen H, Yang Z, Mintier G, Han YH, Chen C, Balimane P, Jemal M, Zhao W, Zhang R, Kallipatti S, Selvam S, Sukrutharaj S, Krishnamurthy P, Marathe P, and Rodrigues AD (2013) Cynomolgus monkey as a potential model to assess drug interactions involving hepatic organic anion transporting polypeptides: in vitro, in vivo, and in vitro-to-in vivo extrapolation. *J Pharmacol Exp Ther* **344:**673-685.

Sirianni GL and Pang KS (1997) Organ clearance concepts: new perspectives on old principles. *J Pharmacokinet Biopharm* **25:**449-470.

Varma MV, Lai Y, Feng B, Litchfield J, Goosen TC, and Bergman A (2012) Physiologically based modeling of pravastatin transporter-mediated hepatobiliary disposition and drug-drug interactions. *Pharm Res* **29:**2860-2873.

Watanabe T, Kusuhara H, Maeda K, Shitara Y, and Sugiyama Y (2009) Physiologically based pharmacokinetic modeling to predict transporter-mediated clearance and distribution of pravastatin in humans. *J Pharmacol Exp Ther* **328:**652-662.

Yamagata T, Zanelli U, Gallemann D, Perrin D, Dolgos H, and Petersson C (2017) Comparison of methods for the prediction of human clearance from hepatocyte intrinsic clearance for a set of reference compounds and an external evaluation set. *Xenobiotica* **47:**741-751.

Yee SW, Brackman DJ, Ennis EA, Sugiyama Y, Kamdem LK, Blanchard R, Galetin A, Zhang L, and Giacomini KM (2018) Influence of Transporter Polymorphisms on Drug Disposition and Response: A Perspective From the International Transporter Consortium. *Clin Pharmacol Ther* **104:**803-817.

Zhang X, Baik J, Jahic M, Jiang W, and Huang Y (2015) In Vitro Evidence of OATP1B1 Induced Drug-Serum Protein Binding Shift and Its Implications on Predicting Drug Clearance and Drug-Drug Interactions. *ISSX workshop: Translating preclinical data to human clearance and pharmacokinetics* **Boston:**October 2016.

Footnote:

Statement of Conflict Interest.

The authors were all employees of Gilead Sciences Inc. during this research and declare no conflicts of interest.

The authors received no outside funding for this work.

DMD Fast Forward. Published on October 9, 2020 as DOI: 10.1124/dmd.120.000163
This article has not been copyedited and formatted. The final version may differ from this version.

Figure captions

Figure 1: The correlation of % free in 100% serum (A) and 10% serum buffer (B) in human and monkey. Sorafenib was excluded in the analysis in 100% serum (A) because it was too highly bound to be experimentally determined.

Figure 2: The correlation of serum protein binding values vs the fold differences of $CL_{u,int\ active}$ or $CL_{u,int\ passive}$ values obtained by normalizing the unbound fraction in the buffer containing 10% serum protein and obtained directly from the uptake with the protein free buffer for OATP substrates.

Figure 3: Curve fitting of pitavastatin I.V. plasma PK in monkey (A) and human (B) using a PBPK model. The open circle represented *in vivo* observed data and the dot-line represented the simulation PK curve. The *in vivo* monkey plasma data was from in-house PK study and human plasma data was digitalized (GetData Graph Digitizer V 2.26.0) from previous published NDA (NDA022363).

Tables

Table 1: Summary of *in vitro* hepatic intrinsic clearance in buffer with and without serum

Human Hepatic Uptake	Serum Free Buffer			Buffer with 10 % Serum			Fold Difference	
Lot: XPM	$CL_{u,int,uptake}$	$CL_{u,int,passive}$	$CL_{u,int,active}$	$CL_{u,int,uptake}$	$CL_{u,int,passive}$	$CL_{u,int,active}$	$CL_{u,int,passive}$	$CL_{u,int,active}$
Asunaprevir	119.7 (52.3)	19.4 (2.9)	100.3	2448.1 (242.4)	154.8 (40.7)	2293.3	8.0	22.9
Atorvastatin	47.9 (2.0)	5 (1.9)	42.9	138.7 (12.3)	7.3 (2.5)	131.4	1.5	3.1
Bosentan	28.5 (12.8)	4.9 (1.2)	23.6	90.9 (12.3)	2.7 (0.3)	88.2	0.6	3.7
Cerivastatin	57.4 (16.1)	5.3 (0.1)	52.1	223.3 (79.3)	10.1 (2.9)	213.3	1.9	4.1
Danoprevir	43 (8.5)	6.2 (2.0)	36.8	167.6 (79.3)	17.1 (5.4)	150.5	2.8	4.1
Fluvastatin	58.7 (36.8)	4.8 (2.9)	53.9	263.4 (45.8)	22.5 (8.6)	240.9	4.7	4.5
Grazoprevir	94.6 (28.6)	12.4 (2.9)	82.2	774.3 (191.1)	34.6 (10.1)	739.7	2.8	9.0
Maraviroc	4.4 (0.08)	0.6 (0.3)	3.8	6.6 (1.8)	0.8 (0.1)	5.8	1.3	1.5
Pitavastatin	50.1 (2.6)	5 (1.2)	45.1	311.0 (37.2)	13.0 (1.9)	298.0	2.6	6.6
Pravastatin	2.3 (0.7)	0.6 (0.2)	1.7	3.4 (1.1)	0.6 (0.04)	2.9	1.0	1.7
Repaglinide	62.3 (18.2)	14.3 (3.9)	48	257.9 (111.6)	10.7 (1.7)	247.1	0.8	5.1
Rosuvastatin	13.5 (2.2)	1.4 (0.7)	12.1	20.1 (1.6)	1.3 (0.1)	18.7	1.0	1.5
Sorafenib	215.9 (67.1)	44.3 (20.6)	171.6	167666.7 (20000.0)	9000.0 (2000.0)	158666.7	203.2	924.6
Telmisartan	156.2 (15.7)	26.8 (5.6)	129.4	1043.8 (300.5)	53.7 (48.3)	990.2	2.0	7.7
Valsartan	7.5 (1.2)	2.3 (0.9)	5.2	105.8 (5.3)	26.5 (5.3)	79.4	11.5	15.3
Monkey Hepatic Uptake	Serum Free Buffer			Buffer with 10 % Serum			Fold Difference	
Lot: UHK	$CL_{u,int,uptake}$	$CL_{u,int,passive}$	$CL_{u,int,active}$	$CL_{u,int,uptake}$	$CL_{u,int,passive}$	$CL_{u,int,active}$	$CL_{u,int,passive}$	$CL_{u,int,active}$
Asunaprevir	205.7 (46.9)	20.7 (4.2)	185	2224.5 (169.9)	76.5 (42.5)	2148.1	3.69	11.61
Atorvastatin	119.7 (10.7)	5.7 (4.2)	114	414.3 (68.5)	7.0 (5.9)	407.3	1.24	3.57
Bosentan	56 (6.4)	3 (0.8)	53	380.2 (46.2)	5.0 (6.4)	375.2	1.67	7.08

Cerivastatin	77.3 (12.9)	4.3 (3.2)	73	415.2 (32.8)	9.6 (7.1)	4056	2.23	5.56
Danoprevir	99.7 (22.3)	5.4 (0.9)	94.3	355.5 (116.0)	6.2 (5.2)	3493	1.15	3.70
Fluvastatin	88 (15.5)	5.4 (1.9)	82.6	265.7 (24.8)	6.4 (1.7)	2594	1.18	3.14
Grazoprevir	156.4 (33.1)	19.8 (2.8)	136.6	1145.1 (488)	36.3 (4.8)	11088	1.83	8.12
Maraviroc	18 (2.0)	0.5 (0.4)	17.5	22.2 (2.9)	0.4 (0.3)	216	0.79	1.25
Pitavastatin	125.4 (17.5)	3.2 (2.3)	122.2	620.1 (103.9)	8.5 (1.7)	6116	2.66	5.00
Pravastatin	7.8 (0.6)	0.5 (0.2)	7.3	8.2 (0.7)	0.7 (0.1)	74	1.48	1.02
Repaglinide	251.8 (37.5)	14.9 (2.3)	236.9	552.8 (230.6)	14.0 (29.1)	5388	0.94	2.27
Rosuvastatin	33.8 (3.7)	1.2 (0.6)	32.6	51.6 (9.8)	1.7 (0.3)	494	1.42	1.53
Sorafenib	241 (66.4)	62.2 (47.9)	178.8	175428.6 (37642.9)	18357.1 (8642.9)	157071.4	295.13	878.48
Telmisartan	313.8 (69.8)	44.1 (15.2)	269.7	2416.3 (167.4)	138.0 (24.1)	22783	3.13	8.45
Valsartan	21.6 (1.9)	1.9 (0.3)	19.7	252.0 (8.1)	8.1 (2.1)	2439	4.28	12.38

1. The *in vitro* uptake clearance was assessed in single donor of human (lot: XPM) and monkey (lot: UHK) hepatocytes. The initial uptake rates were estimated from the slopes of linear uptake phase using linear regression fitting. The experiments were conducted in triplicates for each time point. The mean values were averaged from the triplicates and the standard deviations were presented in the parenthesis. The intrinsic uptake clearance values were calculated by dividing the initial uptake velocity by the nominal substrate concentration. The $CL_{int,active}$ was calculated by subtracting the $CL_{int,passive}$ from $CL_{int,uptake}$. *In vitro* uptake clearance was reported as µl/min/million cells. *In vitro* uptake clearance measured in uptake buffer containing 10% human or monkey serum was normalized the free fraction of protein binding in 10% serum buffer

2. Fold difference = $CL_{u,int}$ in 10% serum buffer/ $CL_{u,int}$ in serum free buffer

Table 2: The *in vitro* to *in vivo* scaling factors estimated for literature compounds

Human	***In Vivo***		**Serum Free Buffer**				**10% Human Serum Buffer**			
L/h	*In* Vivo Fitted Parameters		*In Vitro* Scaled-Up Parameters				*In Vitro* Scaled-Up Parameters			
Compound	$CL_{u,int,passive}$	$CL_{u,int,active}$	$CL_{u,int,passive}$	$CL_{u,int,active}$	SF1 $CL_{u,int,passive}$	SF1 $CL_{u,int,active}$	$CL_{u,int,passive}$	$CL_{u,int,active}$	SF2 $CL_{u,int,passive}$	SF2 $CL_{u,int,active}$
Bosentan	59	8489	65.6	315.9	0.9	26.9	36.1	1189.8	1.6	7.2
Cerivastatin	153	12827	71.0	697.5	2.2	18.4	135.2	2852.6	1.1	4.5
Fluvastatin	147	76513	64.3	721.6	2.3	106.0	301.2	3225.0	0.5	23.7
Pitavastatin	52.6	16071.3	66.9	603.8	0.8	26.6	174.0	3989.5	0.3	4.0
Pravastatin	4.2	406	8.0	22.8	0.5	17.8	8.0	388	0.5	10.5
Repaglinide	1477	13941	191.4	642.6	7.7	21.7	143.2	3308.1	10.3	4.2
Rosuvastatin	1.7	1190	18.7	162.0	0.1	7.3	17.4	256.3	0.1	4.8
Valsartan	23	2463	30.8	69.6	0.7	35.4	354.8	1063.0	0.1	2.3
Median					0.8	24.2			0.5	4.6
Monkey	***In Vivo***		**Serum Free Buffer**				**10% Monkey Serum Buffer**			
L/h/kg	*In Vivo*Fitted Parameters		*In Vitro* Scaled-Up Parameters				*In Vitro* Scaled-Up Parameters			
Compound	$CL_{u,int,passive}$	$CL_{u,int,active}$	$CL_{u,int,passive}$	$CL_{u,int,active}$	SF1 $CL_{u,int,passive}$	SF1 $CL_{u,int,active}$	$CL_{u,int,passive}$	$CL_{u,int,active}$	SF2 $CL_{u,int,passive}$	SF2 $CL_{u,int,active}$
Bosentan	2.1	595.8	0.4	7.8	4.7	76.8	0.7	54.9	2.8	10.8
Pitavastatin	0.2	405.7	0.5	17.9	0.4	22.7	1.2	89.5	0.2	4.5
Rosuvastatin	0.2	52.2	0.2	4.8	0.9	10.9	0.2	7.3	0.6	7.1
Median					0.9	22.7			0.6	7.1

1. *In vivo*-fitted intrinsic clearance in human (except for pitavastatin) was reported previously (Jones et al., 2012)
2. *In vivo*-fitted intrinsic clearance (bosentan and rosuvastatin) in monkey were from Morse et al. (Morse et al., 2017)
3. *In vivo*-fitted intrinsic clearance of Pitavastatin in human and monkey was modeled in house
4. *In vitro*-scaled intrinsic clearance was calculated by *in vitro* uptake clearance X hepatocellularity X liver weigh per body weight. Human is assumed 70 kg body weight

5. SF1 = *in vivo*-fitted value/ *in vitro*-scaled value in serum free buffer; SF2 = *in vivo*-fitted value/ *in vitro*-scaled value in 10% serum buffer

Table 3: Summary of *in vitro* hepatic uptake intrinsic clearance for fifteen OATP substrates

Compound	Human Hepatic Uptake (µl/min/million cells)				Monkey Hepatic Uptake (µl/min/million cells)				Mean Fold Difference	
	Lot	$CL_{u,int,uptake}$	$CL_{u,int,passive}$	$CL_{u,int,active}$	Lot	$CL_{u,int,uptake}$	$CL_{u,int,passive}$	$CL_{u,int,active}$	$CL_{u,int,passive}$	$CL_{u,int,active}$
Asunaprevir	PZA	1283.1 (122.2)	75.4 (20)	1207.7	PNC	1432.0 (292.5)	38.8 (13.3)	1393.2	0.7	1.1
	XPM	2448.1 (242.4)	154.8 (40.7)	2293.3	UHK	2224.5 (169.9)	76.5 (42.5)	2148.1		
	YTW	1460.3 (380.9)	144.6 (79.4)	1315.7	VNV	1776.7 (40.0)	129.9 (36.4)	1646.8		
	Donor mean	1730.5	124.9	1605.6	Donor mean	1811.1	81.7	1729.4		
	Donor SD	627.7	43.2	598.0	Donor SD	397.4	45.7	384.1		
Atorvastatin	PZA	112.5 (27.2)	11.6 (4.0)	100.9	PNC	326.4 (81.5)	8.2 (2.0)	318.2	1.0	3.0
	XPM	138.7 (12.3)	7.3 (2.5)	131.4	UHK	414.3 (68.5)	7.0 (5.9)	407.3		
	YTW	76.2 (8.3)	5.4 (3.8)	70.8	VNV	184.0 (16.1)	8.7 (1.1)	175.3		
	Donor mean	109.1	8.1	101.0	Donor mean	308.2	8.0	300.3		
	Donor SD	31.4	3.2	30.3	Donor SD	116.2	0.9	117.0		
Bosentan	PZA	82.7 (10.8)	3.8 (0.2)	78.9	PNC	175.9 (20.6)	4.5 (2.5)	171.4	1.3	3.3
	XPM	90.9 (12.3)	2.7 (0.3)	88.2	UHK	380.2 (46.2)	5.0 (6.4)	375.2		
	YTW	74.0 (18.5)	5.4 (2.2)	68.6	VNV	242.1 (27.8)	6.7 (4.7)	235.5		
	Donor mean	82.6	4.0	78.6	Donor mean	266.1	5.4	260.7		
	Donor SD	8.4	1.4	9.8	Donor SD	104.2	1.2	104.2		
Cerivastatin	PZA	175.1 (20.2)	9.4 (7.2)	165.7	PNC	311.1 (1.0)	9.1 (3.5)	302.0	1.1	1.9
	XPM	223.3 (79.3)	10.1 (2.9)	213.3	UHK	415.2 (32.8)	9.6 (7.1)	405.6		
	YTW	151.3 (4.3)	5.0 (0.7)	146.3	VNV	312.6 (68.7)	9.1 (1.0)	303.5		
	Donor mean	183.2	8.2	175.1	Donor mean	346.3	9.3	337.0		
	Donor SD	36.7	2.7	34.5	Donor SD	59.6	0.3	59.3		
Danoprevir	PZA	98.1 (20.2)	16.3 (7.4)	81.8	PNC	169.2 (43.0)	13.6 (2.2)	155.6	0.7	2.3
	XPM	167.6 (79.3)	17.1 (5.4)	150.5	UHK	355.5 (116.0)	6.2 (5.2)	349.3		
	YTW	95.4 (4.3)	14.0 (0.7)	81.5	VNV	224.4 (61.4)	15.1 (21.5)	209.3		

	Donor mean	120.4	15.8	104.6	Donor mean	249.7	11.6	238.1		
	Donor SD	40.9	1.6	39.8	Donor SD	95.7	4.8	100.0		
Fluvastatin	PZA	335.1 (56.1)	19.0 (4.8)	316.1	PNC	258.2 (11.6)	9.2 (3.5)	249.0	0.6	1.0
	XPM	263.4 (45.8)	22.5 (8.6)	240.9	UHK	265.7 (24.8)	6.4 (1.7)	259.4		
	YTW	205.5 (21.6)	9.5 (2.6)	196.0	VNV	259.4 (17.3)	16.8 (2.3)	242.6		
	Donor mean	268.0	17.0	251.0	Donor mean	261.1	10.8	250.3		
	Donor SD	64.9	6.7	60.6	Donor SD	4.0	5.4	8.5		
Grazoprevir	PZA	663.7 (145.3)	97.2 (25.7)	566.5	PNC	1175.9 (190.3)	26.0 (9.6)	1149.9	0.5	1.4
	XPM	774.3 (191.1)	34.6 (10.1)	739.7	UHK	1145.1 (488)	36.3 (4.8)	1108.8		
	YTW	733.0 (177.7)	30.2 (14.5)	702.8	VNV	521.6 (119.8)	23.3 (2.7)	498.3		
	Donor mean	723.6	54.0	669.6	Donor mean	947.5	28.5	919.0		
	Donor SD	55.9	37.5	91.2	Donor SD	369.2	6.9	364.9		
Maraviroc	PZA	5.0 (1.1)	0.8 (0.4)	4.2	PNC	33.2 (3.0)	0.7 (1.1)	32.6	0.5	4.2
	XPM	6.6 (1.8)	0.8 (0.1)	5.8	UHK	22.2 (2.9)	0.4 (0.3)	21.8		
	YTW	7.0 (1.2)	1.1 (0.3)	5.9	VNV	13.5 (1.2)	0.4 (0.5)	13.1		
	Donor mean	6.2	0.9	5.3	Donor mean	23.0	0.5	22.5		
	Donor SD	1.0	0.2	1.0	Donor SD	9.9	0.2	9.7		
Pitavastatin	PZA	281.2 (2.0)	16.8 (1.9)	264.4	PNC	477.9 (62.2)	5.1 (0.9)	472.7	0.7	2.0
	XPM	311.0 (37.2)	13.0 (1.9)	298.0	UHK	620.1 (103.9)	8.5 (1.7)	611.6		
	YTW	204.8 (15.5)	11.2 (1.9)	193.7	VNV	451.4 (4.3)	16.2 (11.1)	435.3		
	Donor mean	265.7	13.7	252.0	Donor mean	516.5	9.9	506.5		
	Donor SD	54.7	2.8	53.2	Donor SD	90.7	5.7	92.9		
Pravastatin	PZA	3.1 (0.6)	0.7 (0.7)	2.4	PNC	10.6 (0.4)	0.2 (0.01)	10.4	0.9	3.2
	XPM	3.4 (1.1)	0.6 (0.04)	2.9	UHK	8.2 (0.7)	0.7 (0.1)	7.4		
	YTW	2.7 (0.8)	0.2 (0.2)	2.5	VNV	6.9 (1.4)	0.4 (0.1)	6.6		
	Donor mean	3.1	0.5	2.6	Donor mean	8.6	0.5	8.1		
	Donor SD	0.4	0.2	0.2	Donor SD	1.9	0.3	2.0		
Repaglinide	PZA	224.8 (69.4)	28.1 (3.3)	196.7	PNC	500.0 (78.9)	12.1 (4.9)	487.9	1.0	2.1
	XPM	257.9 (111.6)	10.7 (1.7)	247.1	UHK	552.8 (230.6)	14.0 (29.1)	538.8		

	YTW	177.7 (67.8)	10.7 (1.7)	166.9	VNV	299.2 (169.9)	21.8 (13.3)	277.3		
	Donor mean	220.1	16.5	203.6	Donor mean	450.6	16.0	434.7		
	Donor SD	40.3	10.0	40.5	Donor SD	133.8	5.2	138.6		
Rosuvastatin	PZA	12.8 (0.01)	1.5 (1.3)	11.3	PNC	34.7 (2.6)	0.9 (0.03)	33.8		
	XPM	20.1 (1.6)	1.3 (0.1)	18.7	UHK	51.6 (9.8)	1.7 (0.3)	49.9		
	YTW	15.2 (2.4)	1.0 (0.6)	14.1	VNV	38.9 (4.5)	1.6 (0.7)	37.4	1.1	2.7
	Donor mean	16.0	1.3	14.7	Donor mean	41.7	1.4	40.3		
	Donor SD	3.7	0.2	3.7	Donor SD	8.8	0.5	8.4		
Sorafenib	PZA	110666.7 (3333.3)	4666.7 (2667.7)	106000.0	PNC	279500.0 (43285.7)	21071.4 (13642.9)	258428.6		
	XPM	167666.7 (20000.0)	9000.0 (2000.0)	158666.7	UHK	175428.6 (37642.9)	18357.1 (8642.9)	157071.4		
	YTW	216666.7 (14666.7)	10000.0 (2000.0)	206666.7	VNV	107142.9 (2357.1)	13642.9 (1928.6)	93500.0	2.2	1.1
	Donor mean	165000.0	7888.9	157111.1	Donor mean	187357.1	17690.5	169666.7		
	Donor SD	53050.3	2835.0	50351.4	Donor SD	86795.5	3758.9	83182.6		
Telmisartan	PZA	1133.3 (99.3)	58.1 (19.7)	1075.1	PNC	1943.6 (46.4)	105.7 (23.5)	1837.9		
	XPM	1043.8 (300.5)	53.7 (48.3)	990.2	UHK	2416.3 (167.4)	138.0 (24.1)	2278.3		
	YTW	1292.5 (11.6)	65.3 (9.8)	1227.2	VNV	1935.4 (129.2)	98.6 (81.0)	1836.8	1.9	1.8
	Donor mean	1156.5	59.0	1097.5	Donor mean	2098.5	114.1	1984.3		
	Donor SD	125.9	5.9	120.1	Donor SD	275.3	21.0	254.6		
Valsartan	PZA	84.7 (15.9)	21.2 (4.2)	63.5	PNC	221.1 (21.1)	4.9 (4.0)	216.3		
	XPM	105.8 (5.3)	26.5 (5.3)	79.4	UHK	252.0 (8.1)	8.1 (2.1)	243.9		
	YTW	58.2 (10.6)	15.9 (0.5)	42.3	VNV	154.5 (58.5)	11.4 (11.3)	143.1	0.4	3.3
	Donor mean	82.9	21.2	61.7	Donor mean	209.2	8.1	201.1		
	Donor SD	23.9	5.3	18.6	Donor SD	49.9	3.3	52.1		
								Mean	1.0	2.3

1. The *in vitro* uptake clearance was assessed in three donors of human (lot: PZA, XPM, and YTW) and monkey (lot: PNC, UHK, and VNV) hepatocytes. The initial uptake rates were estimated from the slopes of linear uptake phase using linear

regression fitting. The intrinsic uptake clearance values were calculated by dividing the initial uptake velocity by the nominal substrate concentration. For each donor, the experiments were conducted in triplicates for each time point. The mean values were averaged from the triplicates and the standard deviations (SD) were presented in the parenthesis. Additionally, the donor mean value and the donor SD value for each compound were obtained from the three donors using the mean value of each donor. The $CL_{int,active}$ was calculated by subtracting the $CL_{int,passive}$ from $CL_{int,uptake}$. *In vitro* uptake clearance was reported as µl/min/million cells.

2. *In vitro* uptake clearance measured in uptake buffer containing 10% human or monkey serum was normalized the free fraction of protein binding in 10% serum buffer
3. Fold difference = mean value of data from three monkey hepatocyte lots / mean value of data from three human hepatocyte lots

Table 4: Summary of transporters involved in transporting selected compounds in human

Compound	OATPs	OATs	Other Transporters
Rosuvastatin	1A2, 1B1, 1B3, 2B1	OAT3	NTCP, BCRP, MRP1-5, P-gp
Cerivastatin	1B1, 1B3, 2B1		P-gp, BCRP, MRPs
Fluvastatin	1B1, 1B3, 2B1		NTCP, BCRP, MRP2, P-gp
Pitavastatin	1A2, 1B1, 1B3, 2B1		NTCP, BCRP, MRP3, MRP4, P-gp
Atorvastatin	1A2, 1B1, 1B3, 2B1		NTCP, BCRP, MRP1, MRP2, MRP4, P-gp
Sorafenib	1B1, 1B3		OCT1, MRP2, P-gp
Pravastatin	1A2, 1B1, 1B3, 2B1	OAT3, OAT4, OAT7	NTCP, BCRP, MRP1, MRP2, MRP4, MRP5, BSEP, P-gp
Danoprevir	1B1, 1B3		MRP2, P-gp
maraviroc	1B1		P-gP
bosentan	1B1, 1B3, 2B1		MRP2, P-gp
repaglinide	1B1, 1B3		P-gp
grazoprevir	1B1, 1B3		BCRP, P-gp
telmisartan	1B3, 2B1		
asunaprevir	1B1, 2B1		P-gp
Valsartan	1B1, 1B3	OAT1, OAT3	MRP2, P-gp

The uptake and efflux transporters of each selected compounds are summarized from Drug Interaction Solution Database, University of Washington (https://didb.druginteractionsolutions.org).

Figure 1

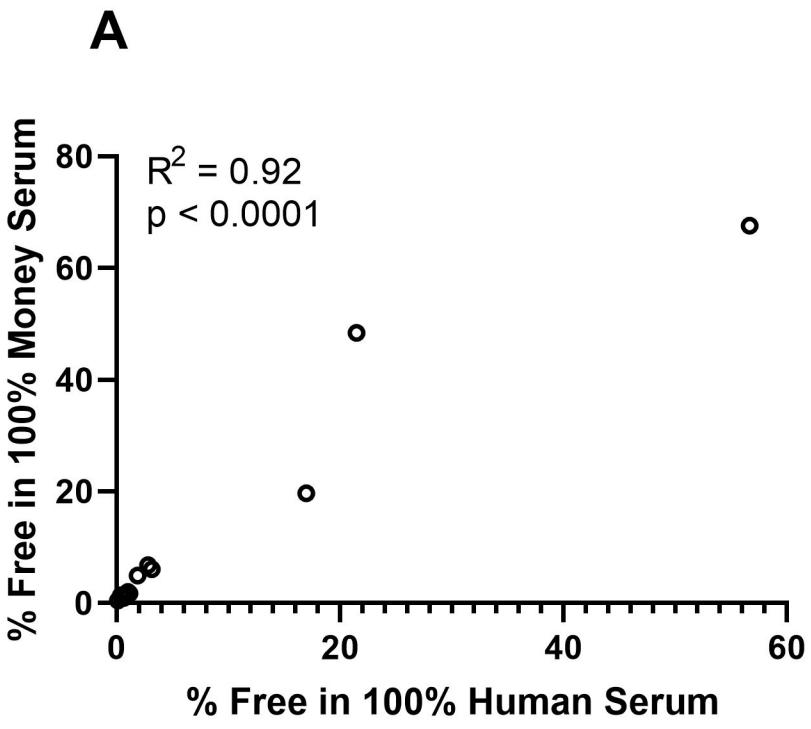

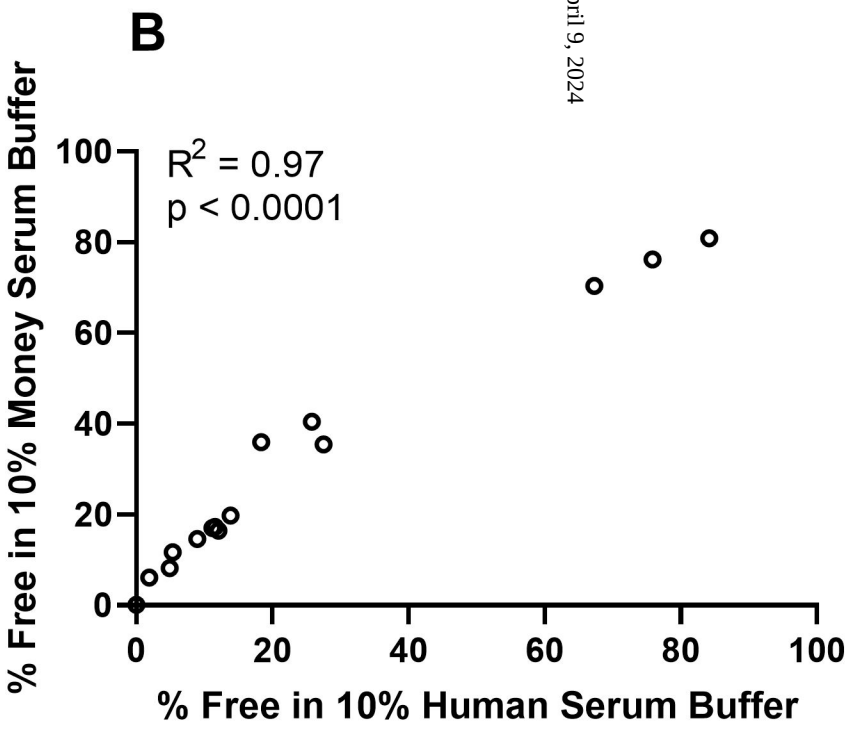

Figure 2

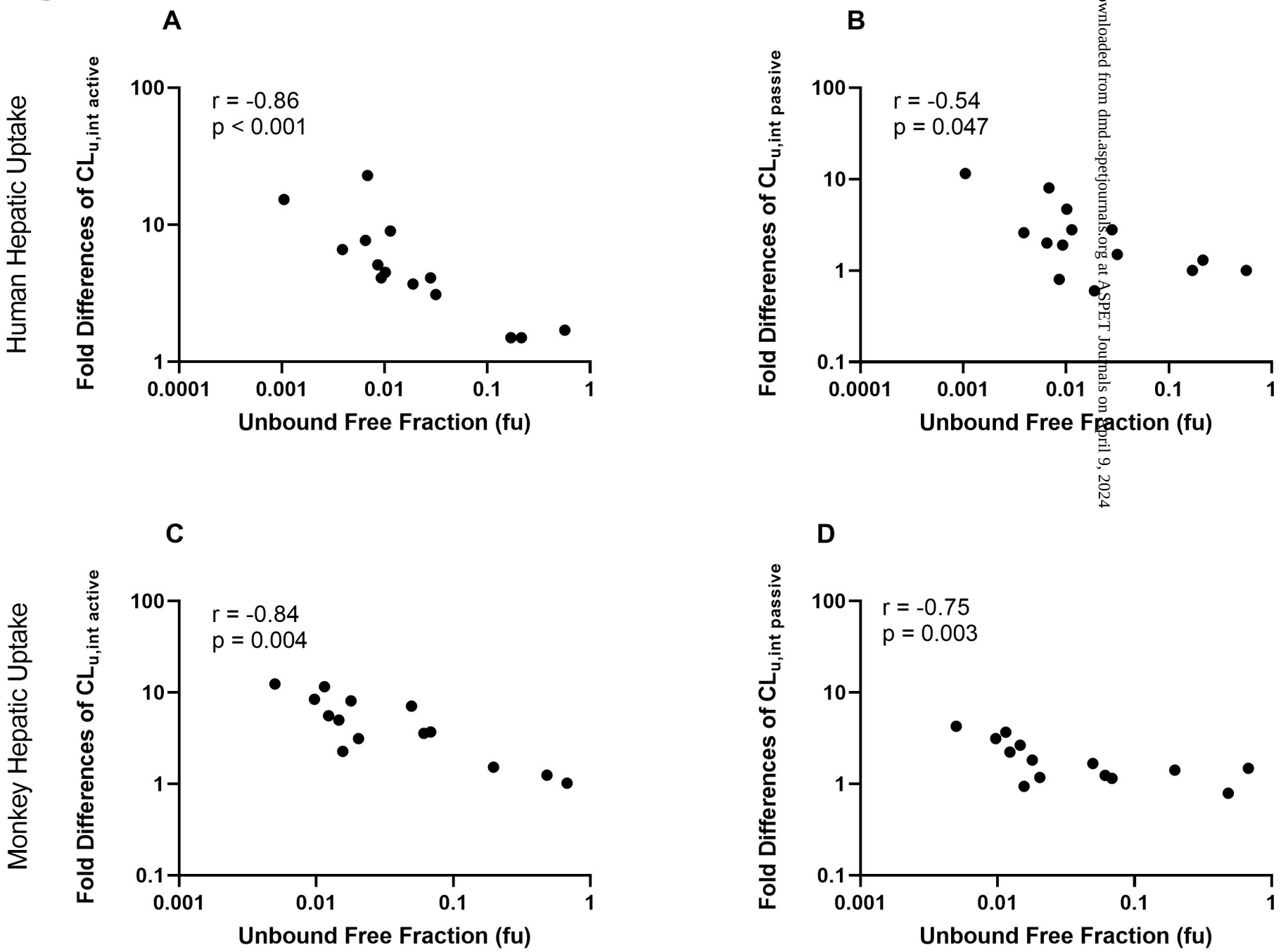

Figure 3

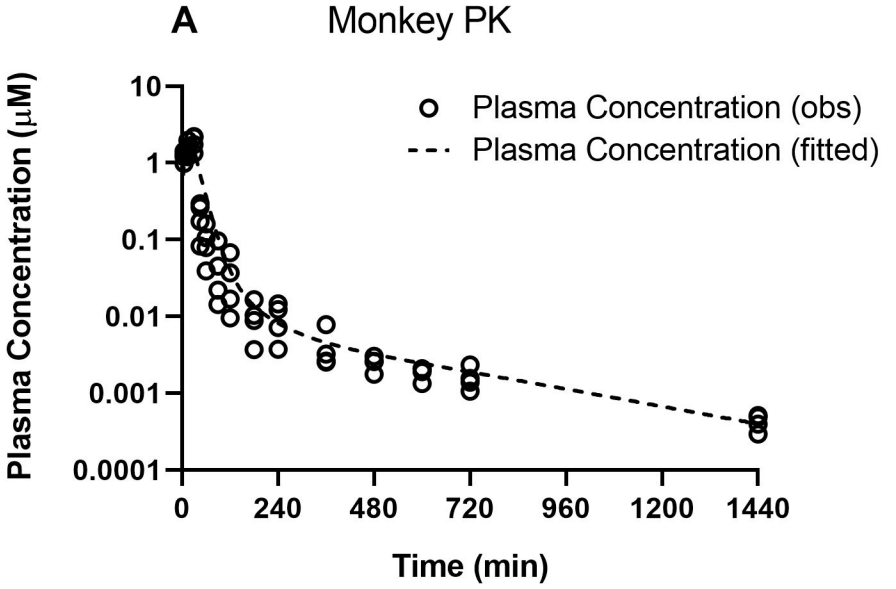
A
Monkey PK
Plasma Concentration (obs)
Plasma Concentration (fitted)
Plasma Concentration (μM)
10
1
0.1
0.01
0.001
0.0001
0
240
480
720
960
1200
1440
Time (min)

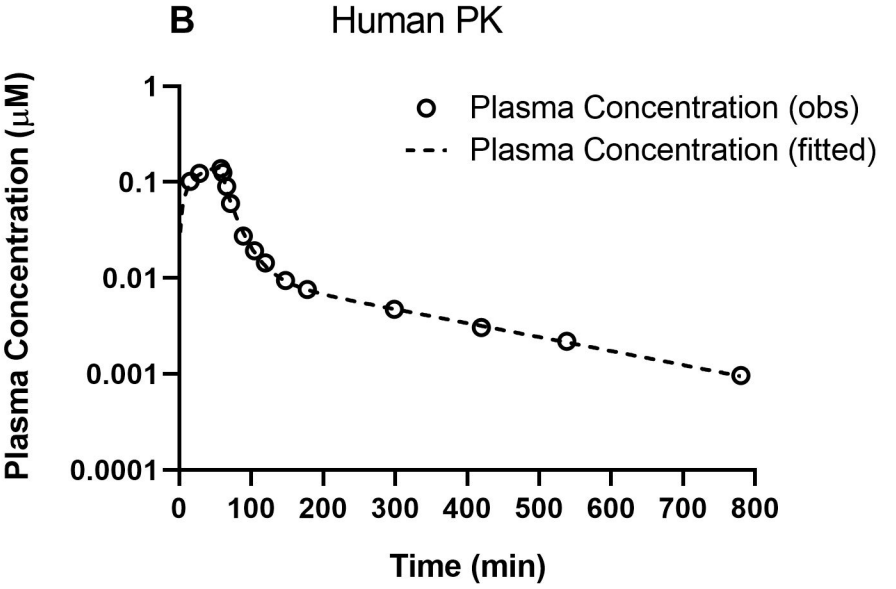
B
Human PK
Plasma Concentration (obs)
Plasma Concentration (fitted)
Plasma Concentration (μM)
1
0.1
0.01
0.001
0.0001
0
100
200
300
400
500
600
700
800
Time (min)

Supplemental materials

Title:
In Vitro Hepatic Uptake in Human and Monkey Hepatocytes in the Presence and Absence of Serum Protein and Its *In Vitro* to *In Vivo* Extrapolation

Authors:
Xiaomin Liang, Yeojin Park, Natalie DeForest, Jia Hao, Xiaofeng Zhao, Congrong Niu, Kelly Wang, Bill Smith and Yurong Lai

Journal: Drug Metabolism and Disposition

DMD-AR-2020-000163

Supplemental Table S1. Human primary hepatocyte donor demographics

Human hepatocytes donor	Donor	Age	Gender	Ethnicity
YTW	Single	19	M	WH
XPM	Single	57	M	WH
PZA	Single	76	M	WH

Supplemental Table S2. Monkey primary hepatocyte donor demographics

Monkey hepatocytes donor	Donor	Gender	Ethnicity
UHK	Single	M	Cynomolgus
VNV	Single	M	Cynomolgus
PNC	Single	M	Cynomolgus

Supplemental Table S3. LC-MS/MS conditions

LC methods

Flow rate	0.6 ml/min
Gradient (B concentration %)	0.2 min 10% B; 1.2 min 99% B; 1.5 min 99% B; 1.55 min 10% B
Mobile phase	A: 1% acetonitrile in water with 0.2% formic acid
	B: 1% water in acetonitrile with 0.2% formic acid

Mass transitions for 15 compounds

Compound	ESI mode	m/z	
Asunaprevir	positive	748.3	648.3
Atorvastatin	negative	559.3	440.2
Bosentan	positive	552.23	202
Cerivastatin	negative	460.3	356.1
Danoprevir	negative	730.3	120
Fluvastatin	negative	412.3	224
Grazoprevir	positive	767.342	646.275
Maraviroc	positive	514.323	389.21
Pitavastatin	negative	422.2	290.1
Pravastatin	negative	423.3	321.2
Repaglinide	positive	453.28	230.138
Rosuvastatin	positive	482.1	258.2
Sorafenib	positive	465.1	252
Telmisartan	positive	515.293	276.087
Valsartan	positive	436.387	207.064

Supplemental Table S4. Protein binding in human and monkey serum

Compound	100% Human Serum		10% Human Serum	
	% Free	% Recovery	% Free	% Recovery
Asunaprevir	0.68	86	4.91	97
Atorvastatin	3.15	101	27.55	101
Bosentan	1.89	97	18.37	102
Cerivastatin	0.93	97	13.88	103
Danoprevir	2.80	92	25.78	103
Fluvastatin	1.02	89	11.58	94
Grazoprevir	1.14	91	8.95	97
Maraviroc	21.48	98	75.85	119
Pitavastatin	0.39	104	5.37	102
Pravastatin	56.69	116	84.17	103
Repaglinide	0.86	99	12.10	106
Rosuvastatin	16.98	105	67.32	110
Sorafenib	N.A.	89	0.03	98
Telmisartan	0.65	98	11.18	97
Valsartan	0.11	102	1.89	105
Compound	**100% monkey Serum**		**10% monkey Serum**	
	% Free	**% Recovery**	**% Free**	**% Recovery**
Asunaprevir	1.15	86	8.24	100
Atorvastatin	6.11	98	35.48	110
Bosentan	4.97	102	35.93	110
Cerivastatin	1.23	93	19.80	114
Danoprevir	6.85	87	40.42	109
Fluvastatin	2.04	88	17.31	100
Grazoprevir	1.79	87	14.61	98
Maraviroc	48.41	127	76.18	115
Pitavastatin	1.46	97	11.74	109
Pravastatin	67.66	107	80.84	110
Repaglinide	1.56	101	16.48	117
Rosuvastatin	19.69	109	70.40	115
Sorafenib	N.A.	87	0.14	92
Telmisartan	0.97	95	17.03	102
Valsartan	0.50	101	6.15	113

(1). The % free of test compound was calculated by the following equation:
% Free = (Peak area ratio of analyte over internal standard in the buffer chamber/ Peak area ratio of analyte over internal standard in the serum chamber) × 100%
(2). The % recovery of test compound was calculated by the following equation:
% Recovery = (Ratio of the peak areas of analyte over internal standard in the buffer chamber*buffer volume + Ratio of the peak areas of analyte over internal standard in the serum

chamber*serum volume)/ (Ratio of the peak areas of analyte over internal standard in the T0 sample*serum volume) × 100%
(3). N.A.: not applicable. The binding of sorafenib in 100 % serum cannot be experimentally determined due to highly protein bound.
(4) Data was presented as mean of duplicates.

Supplemental Figures

Supplemental Figure S1. The time-course profile for the hepatic uptake. The error bars were represented standard deviation of triplicates.

A. Hepatic uptake of human PZA lot hepatocytes in 10% serum buffer

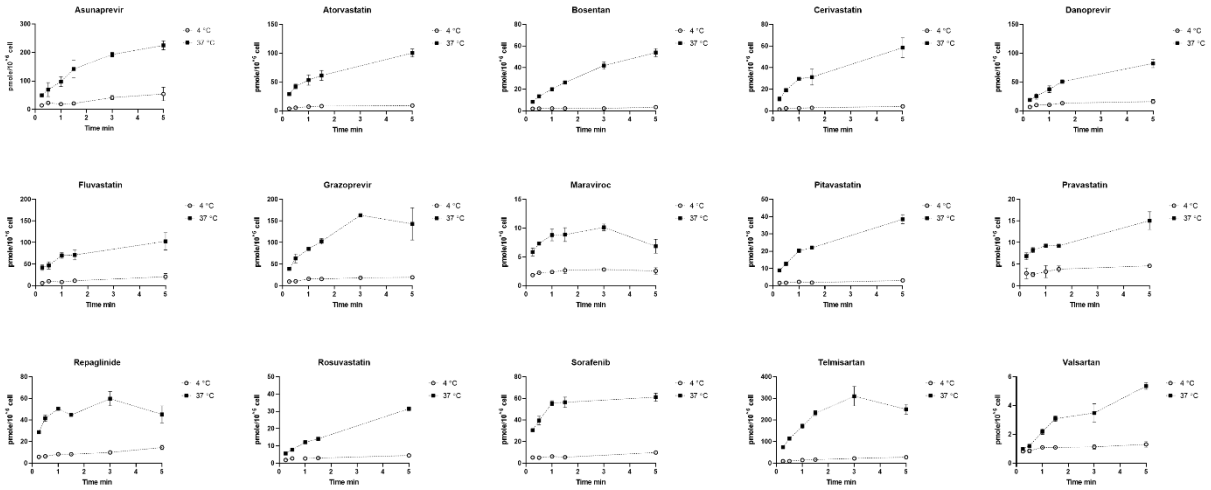

B. Hepatic uptake of human XPM lot hepatocytes in 10% serum buffer

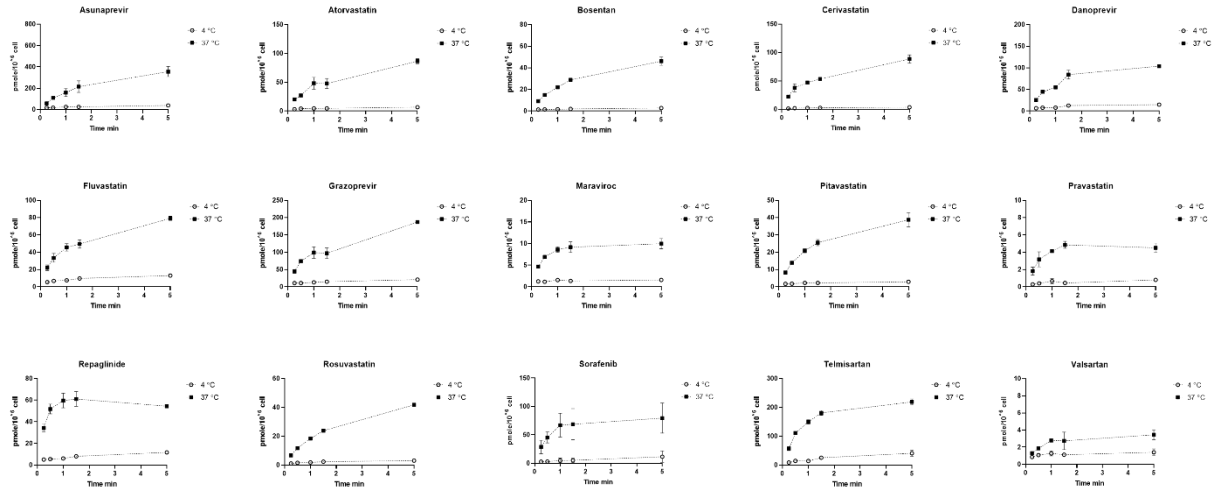

C. Hepatic uptake of human YTW lot hepatocytes in 10% serum buffer

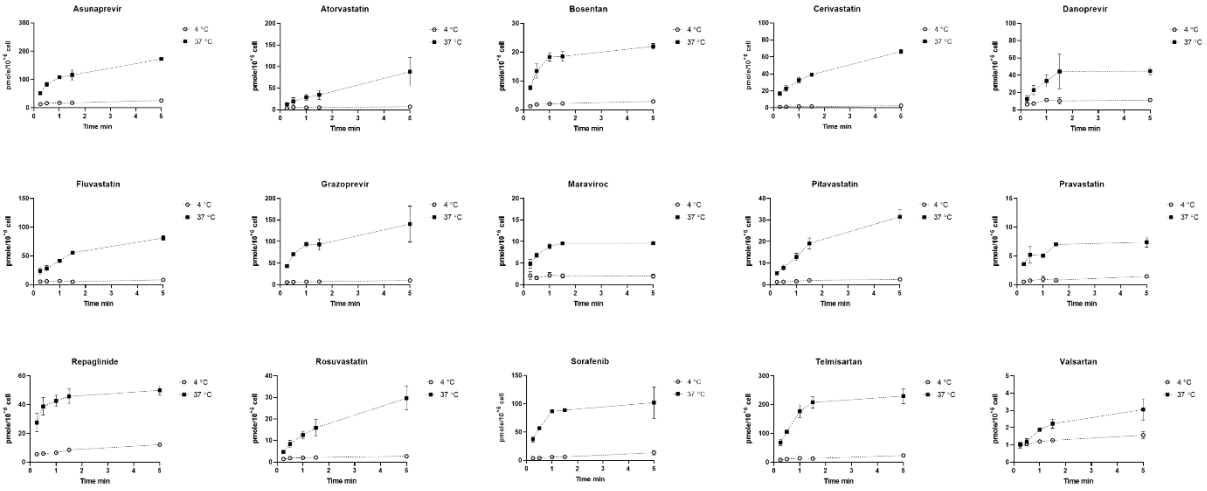

D. Hepatic uptake of monkey PNC lot hepatocytes in 10% serum buffer

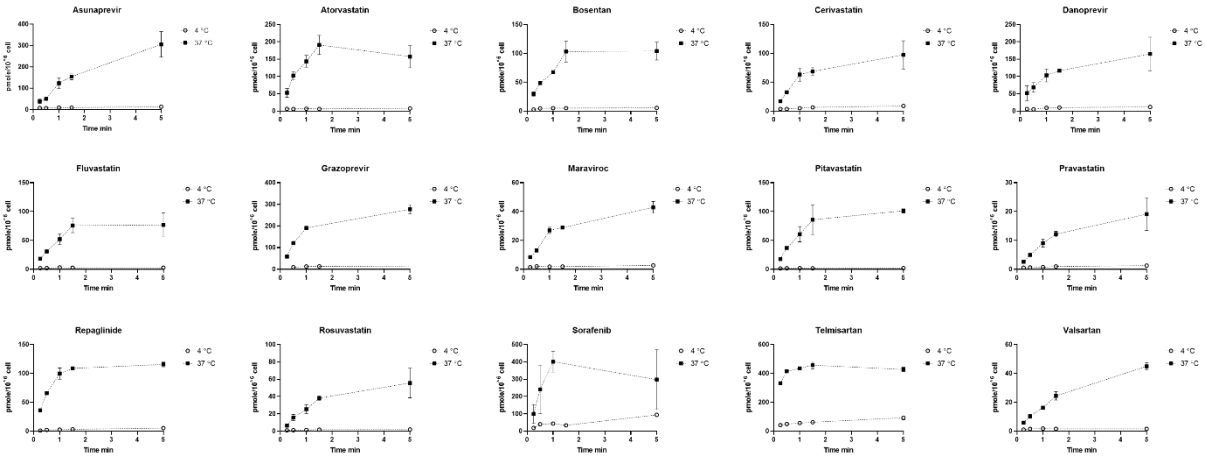

E. Hepatic uptake of monkey UHK lot hepatocytes in 10% serum buffer

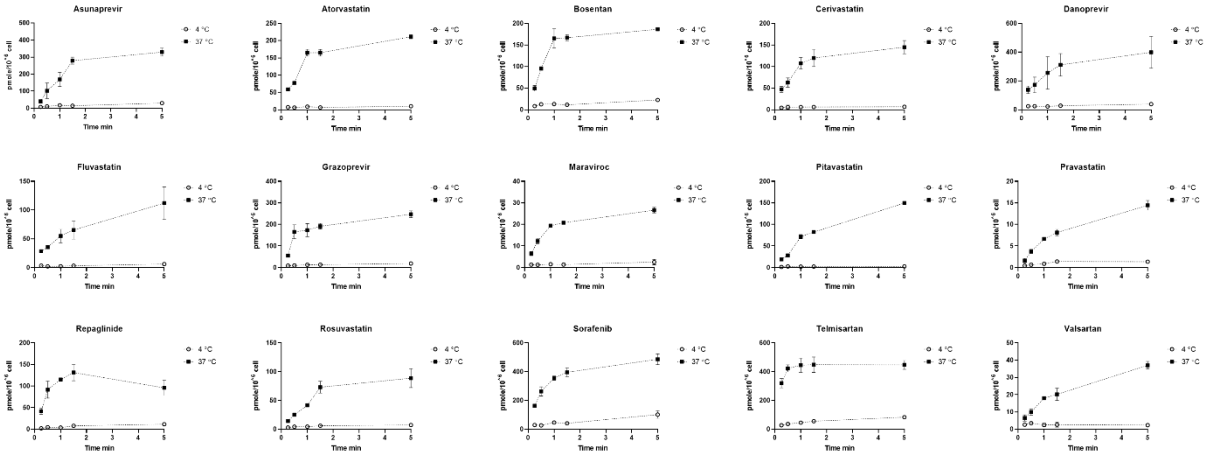

F. Hepatic uptake of monkey VNV lot hepatocytes in 10% serum buffer

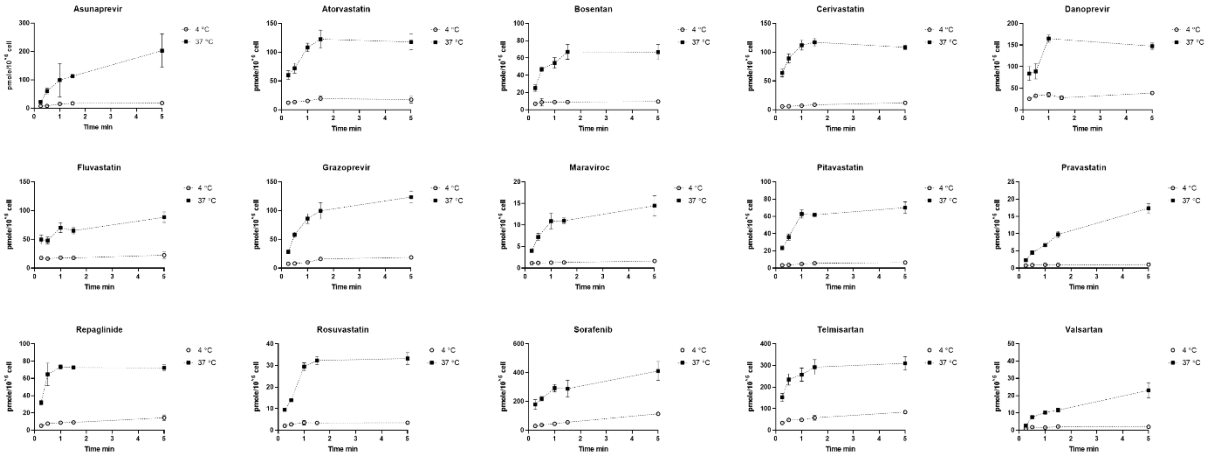

G. Hepatic uptake of human XPM lot hepatocytes in serum free buffer

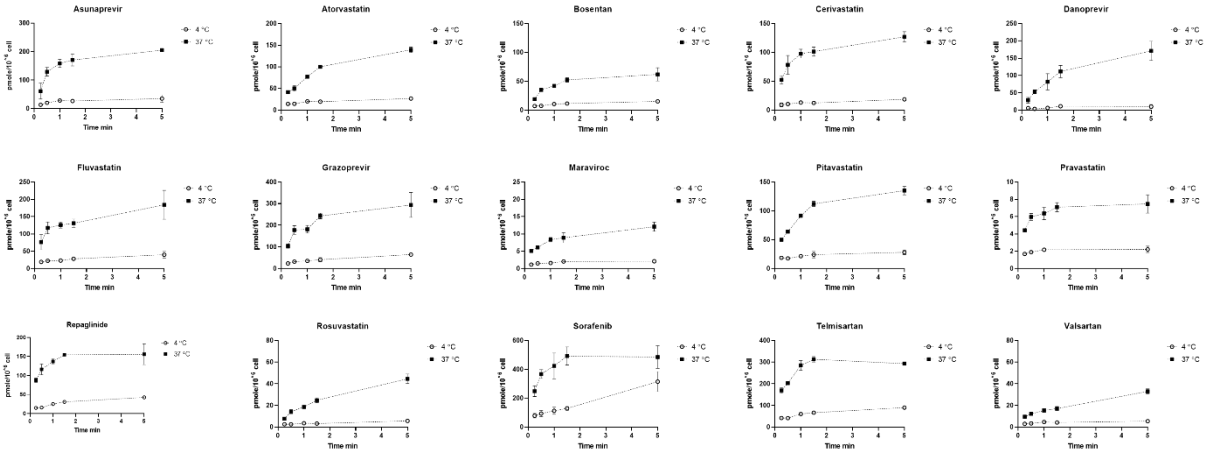

H. Hepatic uptake of monkey UHK lot hepatocytes in serum free buffer